J Nanostruct 13(2): 587-596, Spring 2023

RESEARCH PAPER

Synthesis and Characterization of Chitosan-Grafted-Poly(Acrylic Acid)/Kaolin Nanocomposite for Adsorption of Malachite Green from Aqueous Solutions: Application of Thermodynamic and Isotherm Models

Ahmed S. Abbas [1], Duha M. Eidan [2], Makarim A. Mahdi [2] and Layth S. Jasim [2]*

[1] *Department of Chemistry, College of Science, University of Babylon, Hilla, Iraq*

[2] *Department of Chemistry, College of Education, University of Al-Qadisiyah, Diwaniyah, Iraq*

ARTICLE INFO

Article History:
Received 19 January 2023
Accepted 27 March 2023
Published 01 April 2023

Keywords:
Adsorption
Chitosan
Hydrogels
Kaolin
Malachite green
Nanocomposite

ABSTRACT

In an in-depth study of Malachite Green (MG) dye adsorption on a chitosan-graft-poly(acrylic acid)/Kaolin (CS-g-P(AA)/Kaolin) nanocomposite, FTIR, FE-SEM, and adsorption isotherm analysis revealed significant findings. A pronounced decrease in absorption bands associated with amino and hydroxyl groups suggested their active involvement in dye sorption through hydrogen bonding. Post-adsorption FE-SEM images showed a roughened surface, indicating dye adsorption. The study carefully examined the effect of adsorbent weight on MG adsorption and found that surface saturation reduced adsorption efficiency beyond 0.05 gm. To maximise dye removal efficiency, adsorbent weight must be balanced. The Freundlich isotherm model favoured multilayer adsorption on heterogeneous surfaces, as demonstrated by a stronger correlation coefficient (R^2= 0.9448) compared to Langmuir and Temkin models. Enhanced kinetic energy and entropy caused increased adsorption at higher temperatures, suggesting a largely physical adsorption process. Positive enthalpy (ΔH) and entropy (ΔS) changes in thermodynamic analysis support physical bonding, while positive Gibbs free energy (ΔG) indicates non-spontaneous adsorption. Conclusions show that CS-g-P(AA)/Kaolin can remove MG dye, and that adsorbent weight, surface contacts, and temperature are crucial. The findings help optimise adsorption techniques for environmental remediation, notably dye pollution management, demonstrating a scientific approach to dealing with environmental issues.

How to cite this article
Abbas A. S., Eidan D. M., Mahdi M.A., Jasim L. S. Synthesis and Characterization of Chitosan-Grafted-Poly(Acrylic Acid)/Kaolin Nanocomposite for Adsorption of Malachite Green from Aqueous Solutions: Application of Thermodynamic and Isotherm Models. J Nanostruct, 2023; 13(2):587-596. DOI: 10.22052/JNS.2023.02.029

INTRODUCTION

In the near future, substantial costs are anticipated for mitigating damages caused by industrial activities and technological advancements [1]. Currently, dyes find diverse applications across various industries [2]. However, many of these dyes pose carcinogenic and mutagenic risks to humans and other organisms [3]. Malachite green, a triphenylmethane chemical structure dye, is extensively used in the aquaculture industry against external parasites, fungus, and bacteria [4]. It is also utilized in the dyeing industries for

* *Corresponding Author Email: sci.ahmed.saadoon@uobabylon.edu.iq*

materials like silk, wool, jute, hemp, and paper [5]. Despite its effectiveness in controlling infections from bacteria, protozoa, nematodes, trematodes, and cestodes in aquaculture, malachite green is toxic and can induce liver tumors in standard organisms [6, 7]. Excessive use of malachite green, due to its detrimental environmental impact and health threats to organisms, necessitates urgent attention [8]. Conventional physicochemical methods, including chemical precipitation, solvent extraction, ion exchange resins, and others, have been employed to remove malachite green and other harmful organic compounds from water [9]. Given the molecular structure and aromatic complex of dyes, they are generally resistant to degradation by light, biological activities, oxidizing agents, and other environmental conditions [10, 11]. Consequently, traditional biological water purification systems are ineffective against dyes [12]. Moreover, these methods have disadvantages like incomplete removal of malachite green, high costs, and the need for extensive monitoring, energy, chemical consumption, and toxic sludge production [13]. This natural material exists in various forms, with Kaolin and smectite being the most commonly used in the industry. Kaolin has a platy structure resembling gold (metal leaf) with the chemical formula $Al_2Si_2O_5(OH)_4$, consisting of hexagonal or octagonal sheets [14]. These sheets or plates are composed of linked silicon-oxygen tetrahedra forming hexagonal rings. By repeating these rings in two dimensions, a sheet or plate is formed. Octahedral sheets are made up of silicon and aluminum units [15]. The Kaolin layer structure, is held together by hydrogen bonds between hydroxyl groups in the octahedral sheets and oxygen in the tetrahedral sheets [16]. Hydrogels, crosslinked polymers, can be synthesized either physically or chemically, contingent upon the type of polymer and the specific experimental conditions [17]. Physical crosslinking is deemed environmentally benign, owing to its independence from cross-linking agents or initiators [18]. Conversely, chemical methods, involving covalent bond formation, result in hydrogels characterized by greater stability and augmented mechanical strength [19]. Chitosan, sourced from the alkaline deacetylation of chitin (the second most plentiful natural polymer following cellulose), presents advantageous properties for material development [20]. These include biocompatibility, biodegradability, cost-effectiveness, and high reactivity attributed to Multiple functional groups [21]. Thus, chitosan Surface as a superior candidate for fabricating nanocomposite hydrogels aimed at the adsorption of MG dye [22]. The Adoption of synthetic polymers into these natural material-based hydrogels further amplifies their desired physical and chemical characteristics [23].

In aqueous solutions, hydrogel/Kaolin clay was tested for hazardous MG cation adsorption. MG removal efficiency was affected by starting MG ion concentrations, adsorbent dose, and temperature. Kinetic, mechanistic, and thermodynamic investigations were also performed to understand MG-adsorbent interactions and find the best mathematical models for adsorption. The study also reactivated the adsorbent's surface for recurrent use during removal.

MATERIALS AND METHODS

Preparation of CS-g-P(AA)/Kaolin nanocomposite

The CS-g-P(AA)/Kaolin hydrogel nanocomposite was prepared from a series of solutions starting with the dissolution of 1.0 g of chitosan (CS) in 40 mL of 1% acetic acid, stirred using a magnetic stirrer (hotplate stirrer) for 15 minutes. Subsequently, 10 mL of acrylic acid (AA) was added, followed by varying amounts (0.5, 1, 1.5, 2 grams) of the primary material, Kaolin clay (KAOLIN), dissolved in 10 mL of distilled water with continuous stirring for 30 minutes. Additionally, a cross-linker solution of MBA was prepared by dissolving 0.05 g in 2 mL of distilled water. Then, a solution of potassium persulfate (KPS) was prepared by dissolving 0.05 g in 2 mL of distilled water with continuous stirring. Nitrogen gas was then injected for a minute, after which the prepared solution was transferred to test tubes and then to a water bath at 70°C for 2 hours to complete the reaction. The nanocomposite was then cut, washed with distilled water, and dried in an electric oven at a temperature of 70°C, as shown in Fig.1.

CS-g-P(AA)/Kaolin nanocomposite characterization

Fourier transform infrared (FTIR) spectroscopy

In attenuated reflection setting, the synthesized CS-g-P(AA)/Kaolin hydrogels' chemical structures were checked out making use of a Range GX FTIR System (Perkin-Elmer, United States). The FTIR ranges, covering wavenumbers from 400 to 4000 cm^{-1}, were acquired from 64 scans at a resolution of 2 cm^{-1}.

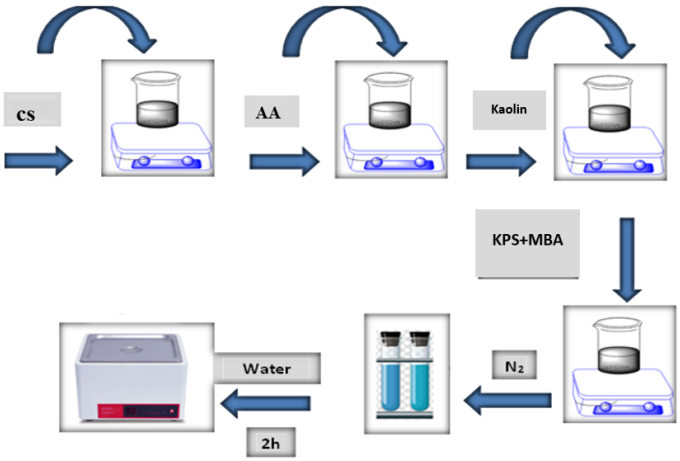

Fig. 1. Schematic diagram of stag of CS-g-P(AA)/Kaolin nanocomposite preparation

Scanning electron microscope (SEM)

The JEOL JSM-6510LV SEM from Japan was utilized to catch the cross-sectional shape of the manufactured hydrogels. Before the SEM evaluation, the hydrogels were dried out using a lyophilizer under vacuum conditions. After drying, they were coated with platinum. The ImageJ software application was utilized to identify the ordinary sizes of pores in each group of hydrogels by analyzing 100 pores from an SEM image.

Adsorption Isotherm

In this procedure, 10 mL solutions of MG with concentrations ranging from 50 to 500 ppm were introduced into stoppered flasks containing 0.05 g of chaff. These flasks were then agitated in a thermostatically controlled water bath at a speed of 120 rpm until equilibrium was reached, which was 150 minutes for MG. These durations were sufficient to allow the adsorption process to reach equilibrium in case. Following the lapse of the equilibrium time, the suspensions were centrifuged at 6000 rpm for 20 minutes. The resultant clear supernatants were then analyzed for dye content, after suitable dilution, using a UV-visble Spectrophotometer (FAAS). Equilibrium concentrations were determined by comparing the experimental data with a pre-established calibration curve.

The equation 1 for determining the removal capacity (qe) at equilibrium is given by:

$$q_e = \frac{Vsol.(Co - Ce)}{m} \quad (1)$$

$$\% E = \frac{(Co - Ce)}{Co} x100 \quad (2)$$

Here, qe (expressed in mg/g) represents the amount of MG adsorbed per unit mass of the adsorbent at equilibrium. C_o and C_e are the initial and equilibrium concentrations of MG in the solution (in mg/L), respectively. V_{sol} is the volume of the solution (in Liters), and m is the mass of the adsorbent used (in grams). In this equation (2), %E represents the efficiency of adsorption in percentage. These equations are fundamental in evaluating the effectiveness of the adsorbent in removing specific dye from a solution, providing a quantitative measure of the adsorption process.

Effect of Temperature

For the thermodynamic aspect of adsorption, the experiment was replicated at different temperatures (25°C, 40°C, and 55°C) to evaluate the fundamental thermodynamic functions. This approach helps in understanding how temperature variations impact the adsorption process and allows for the calculation of thermodynamic parameters such as enthalpy, entropy, and Gibbs free energy changes.

RESULTS AND DISCUSSION

Characterization

The FTIR spectra of MG-loaded adsorbent CS-g-P(AA)/Kaolin were analyzed, as shown in Fig. 2. Compared to the surface spectra of CS-g-P(AA)/KAOLIN, a notable decrease in the broad absorption bands at 3300 and 3450 cm^{-1} was

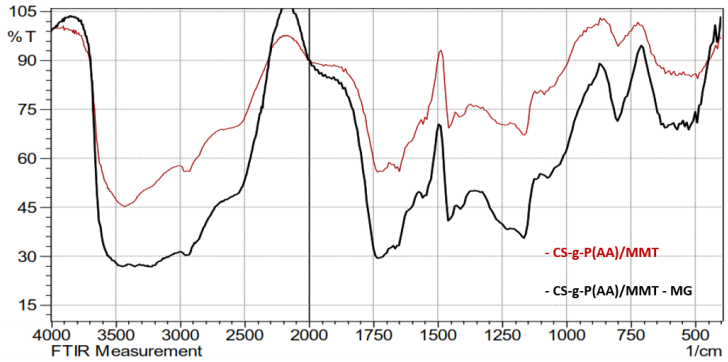

Fig. 2. FTIR analysis of CS-g-P(AA)/Kaolin and CS-g-P(AA)/Kaolin - MG

observed. This change in intensities, particularly in the amino and hydroxyl groups' bands, suggests their involvement in dye sorption. This coincides with the formation of hydrogen bonds between the dye and the adsorbent surface, resulting in the disappearance of certain bands previously present on the surface within the confined region of 1600-1000 cm^{-1} [24,25].

The morphology of CS-g-P(AA)/Kaolin before adsorption was examined using FE-SEM, depicted in Fig. 3. The FE-SEM analysis revealed that CS-g-P(AA)/Kaolin tends to form multilayer agglomerates. Post-adsorption, the FE-SEM images showed a roughened CS-g-P(AA)/Kaolin surface with MG evenly dispersed as bright dots, indicating the presence of both CS-g-P(AA)/Kaolin and MG [26,27].

Effect of Adsorbent Weight on the Adsorption process

10mL of a MG solution at a fixed concentration of 100 ppm were added to the aforementioned weights of the nanocomposite at a temperature of 20°C. The study results, as illustrated in Fig. 4, indicate that an increase in the weight of the adsorbing surface leads to an increase in the adsorption amount. This is attributed to the initial requirement of equilibrium between the adsorbate and adsorbent, ensuring all the active sites of the adsorbent are occupied, which stabilizes the adsorption process on the surface [27]. The maximum adsorption quantity is achieved at 0.05 gm, representing the adsorbent's saturation stage. However, further increase in the adsorbent's weight may result in an unstable dispersion of the large nanocomposite surface compared to the adsorbate (dye) quantity. Consequently, the solute's energy overpowers the adsorption

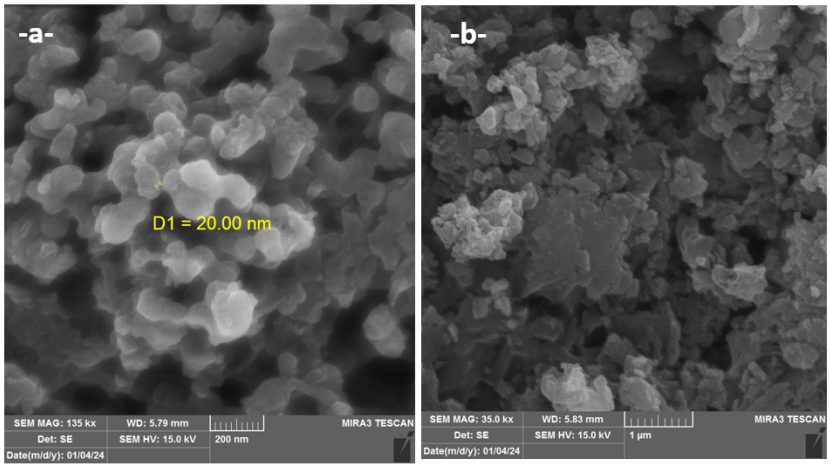

Fig. 3. SEM images of a- CS-g-P(AA)/Kaolin and b- CS-g-P(AA)/Kaolin - MG

energy on the surface, leading to a decrease in the adsorbed quantity on the nanocomposite surface [28].

Adsorption isotherms

The research revealed a stronger correlation with Freundlich isotherms relative to Temkin and Langmuir isotherms, as indicated by the correlation coefficient values (R^2= 0.9448 for Freundlich). This finding was distinctly illustrated in Fig. 5. Additionally, Table 1 provides the correlation coefficients and constants for each isotherm at a temperature of 25°C.

Effect of Temperature on the Adsorption Process

Temperature significantly influences the adsorption process, as changes in temperature affect the adsorptive capacity of the surface for the dye from its aqueous solution. By studying adsorption at various temperatures (10-25°C), the thermodynamic functions of the adsorption process can be understood. The results indicated that the amount of MG adsorbed on the nanocomposite surface increases with an increase in temperature, suggesting that the adsorption process is endothermic [29,30], as illustrated in Fig. 6.

This increase in adsorption with increasing temperature could be absorption into the surface will occur due to the increase in kinetic energy of the dye particles. This increase in temperature leads to a rise in the system's entropy (ΔS), enhancing the randomness of the adsorbed dye molecules on the adsorbent surface. Consequently, the attraction forces between the dye molecules and the available active sites for adsorption on the nanocomposite surface stronger. The enthalpy change (ΔH) value is instrumental in discerning the interaction forces between the adsorbed dye molecules and the adsorbent surface. For ascertaining ΔH, a plot of the natural logarithm of the equilibrium constant (lnK) against the reciprocal of absolute temperature (1/T) is constructed, yielding a linear relationship. The slope of this

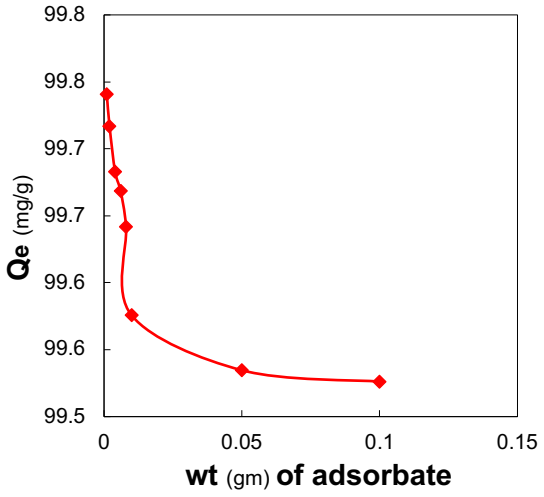

Fig. 4. Effect of the weight of CS-g-P(AA)/Kaolin nanocomposite

Table 1. Langmuir, Freundlich and Temkin isotherm constants for MG uptake by CS-g-P(AA)/KAOLIN

Langmuir equation			Freundlich eq.			Temkin eq.		
$K_{L\ (L/mg)}$	$q_{m\ (mg/g)}$	R^2	K_F	n	R^2	$K_{T\ (L/g)}$	$B_{(J/mol)}$	R^2
0.317	105.263	0.7619	19.552	1.572	0.9448	0.745	23.387	0.8037

graph, equating to (-ΔH/R) and intercept equating to (ΔS/R) facilitates the determination of the enthalpy value associated with the adsorption of MG on the adsorbent polymeric nanocomposite surface [31,32]. This is documented in Table 2 and illustrated in Fig. 7.

The thermodynamic functions presented in the table indicate an endothermic adsorption

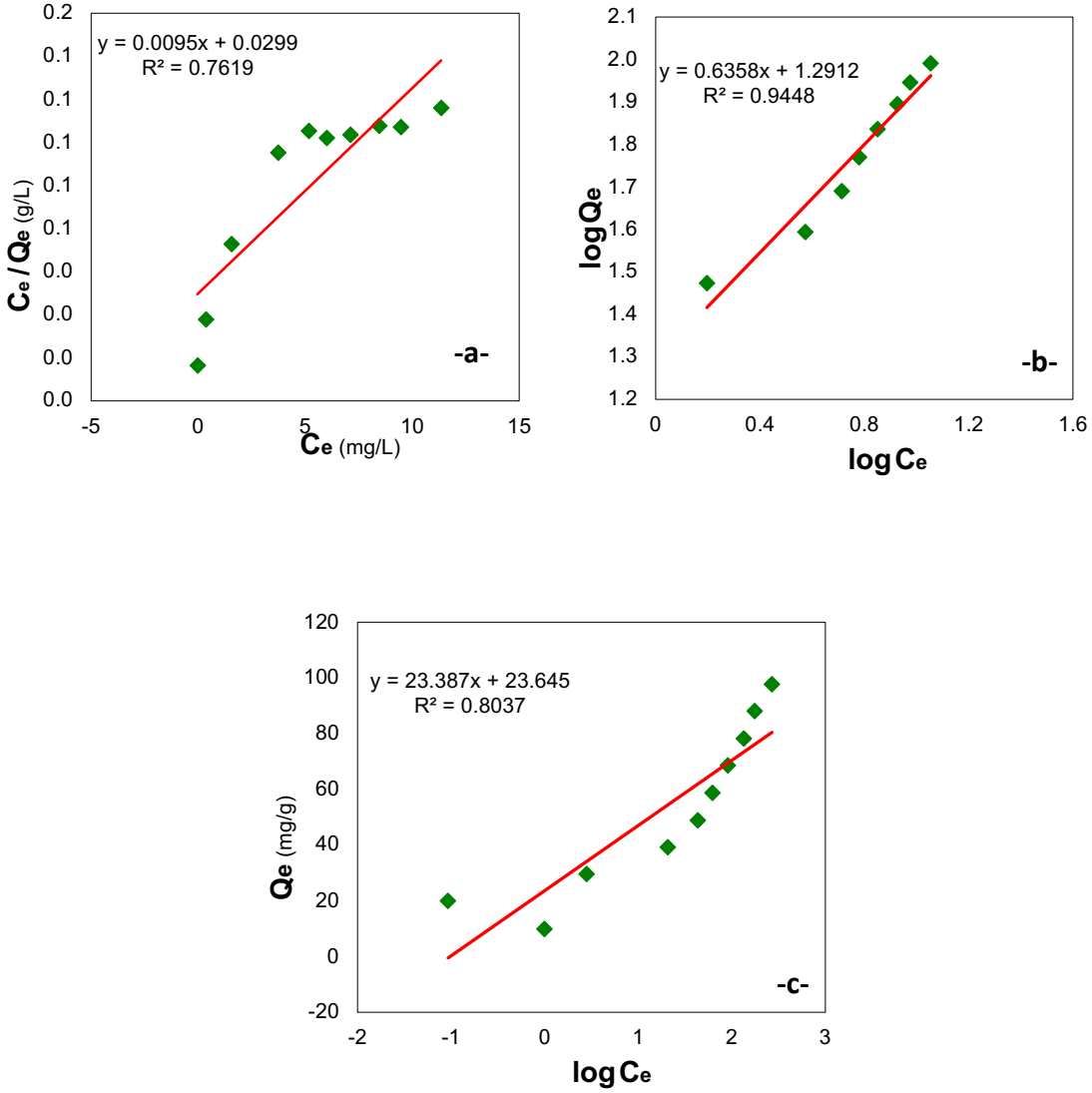

Fig. 5. Langmuir (A), Freundlich (B) and Temkin(C) isotherms of MG adsorption on the CS-g-P(AA)/Kaolin

Table 2. Effect of temperature on the maximum adsorbed quantity for adsorption of MG

$T_{(K)}$	$1/T_{(K)}$	C_o	C_e	q_e	q_e/C_e	ln q_e/C_e	Slope	Intercept
283	0.00353	900	23.62201	95.275	4.0	1.394	-4088.6	15.934
288	0.00347		15.02396	96.995	6.5	1.865		
293	0.00341		13.13398	97.373	7.4	2.003		
298	0.00336		11.35049	97.729	8.6	2.152		

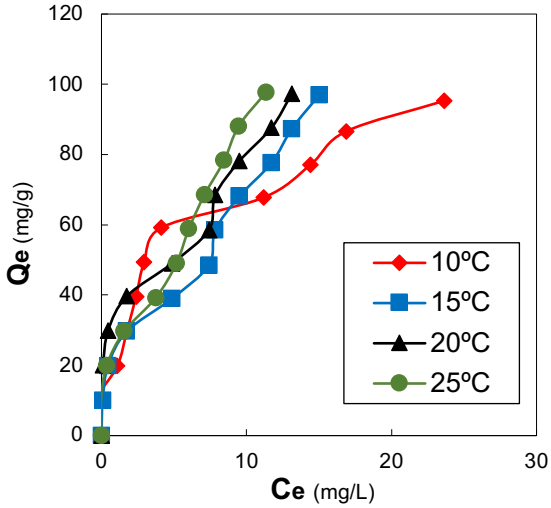

Fig. 6 Effect of Temperature on adsorption MG

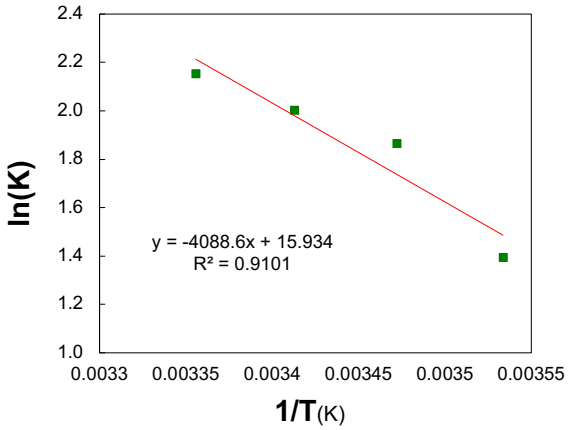

Fig. 7. Plot of ln K against reciprocal absolute temperature for adsorption of MG on CS-g-P(AA)/Kaolin

Table 3. Thermodynamic parameters of adsorption of MG on CS-g-P(AA)/Kaolin surface

$T_{(K)}$	ΔH^0(KJ/mol)	ΔS^0(J/mol. K)	$\Delta G^0(\frac{KJ}{mol})$
298	-18.082	-62.218	0.148

process, as evidenced by the positive enthalpy change (ΔH). This endothermic nature suggests the likelihood of physical bonding, particularly if ΔH is less than 40 KJ/mol. Moreover, the positive entropy change (ΔS) signifies a higher degree of disorder within the system, often associated with restricted molecular movement. Furthermore, the positive Gibbs free energy (ΔG) reinforces this understanding, confirming that the adsorption process is non-spontaneous [33,34].

CONCLUSION

The study presents a comprehensive analysis of the adsorption of MG dye using the CS-g-P(AA)/Kaolin adsorbent. FTIR and FE-SEM results demonstrate significant functional group activity and morphological changes in the adsorbent post-adsorption, indicating effective dye removal.

Adsorption increases with the adsorbent weight, peaking at 0.05 gm, beyond which a decrease in efficiency is observed due to adsorbent surface saturation. The adsorption process aligns closely with Freundlich isotherms, suggesting a multilayer adsorption pattern. Additionally, the adsorption is endothermic, with increasing temperatures enhancing the process. This is supported by positive enthalpy and entropy changes, highlighting the physical nature of the adsorption. The study also underscores the importance of adsorbent-adsorbate equilibrium in optimizing the adsorption process, as well as the role of surface area and active sites in adsorbent effectiveness.

CONFLICT OF INTEREST

The authors declare that there is no conflict of interests regarding the publication of this manuscript.

REFERENCES

1. Chauhan PR, Kaushik SC, Tyagi SK. Current status and technological advancements in adsorption refrigeration systems: A review. Renewable and Sustainable Energy Reviews. 2022;154:111808.
2. Osagie C, Othmani A, Ghosh S, Malloum A, Kashitarash Esfahani Z, Ahmadi S. Dyes adsorption from aqueous media through the nanotechnology: A review. Journal of Materials Research and Technology. 2021;14:2195-2218.
3. Kausar A, Zohra ST, Ijaz S, Iqbal M, Iqbal J, Bibi I, et al. Cellulose-based materials and their adsorptive removal efficiency for dyes: A review. Int J Biol Macromol. 2023;224:1337-1355.
4. Gharavi-nakhjavani MS, Niazi A, Hosseini H, Aminzare M, Dizaji R, Tajdar-oranj B, et al. Correction to: Malachite green and leucomalachite green in fish: a global systematic review and meta-analysis. Environmental Science and Pollution Research. 2023;30(17):48928-48928.
5. Akköz Y, Coşkun R. Preparation of highly effective bio-adsorbent from hemp fiber for removal of malachite green oxalate (MGO). Cellulose. 2023;30(7):4511-4525.
6. Majeed SA, Nambi KSN, Taju G, Vimal S, Venkatesan C, Hameed ASS. Cytotoxicity, genotoxicity and oxidative stress of malachite green on the kidney and gill cell lines of freshwater air breathing fish Channa striata. Environmental Science and Pollution Research. 2014;21(23):13539-13550.
7. Srivastava S, Sinha R, Roy D. Toxicological effects of malachite green. Aquat Toxicol. 2004;66(3):319-329.
8. Raval NP, Shah PU, Shah NK. Malachite green "a cationic dye" and its removal from aqueous solution by adsorption. Applied Water Science. 2016;7(7):3407-3445.
9. Dahri MK, Kooh MRR, Lim LBL. Water remediation using low cost adsorbent walnut shell for removal of malachite green: Equilibrium, kinetics, thermodynamic and regeneration studies. Journal of Environmental Chemical Engineering. 2014;2(3):1434-1444.
10. Roy M, Saha R. Dyes and their removal technologies from wastewater: A critical review. Intelligent Environmental Data Monitoring for Pollution Management: Elsevier; 2021. p. 127-160.
11. Selvaraj V, Swarna Karthika T, Mansiya C, Alagar M. An over review on recently developed techniques, mechanisms and intermediate involved in the advanced azo dye degradation for industrial applications. J Mol Struct. 2021;1224:129195.
12. Bhatia D, Sharma NR, Singh J, Kanwar RS. Biological methods for textile dye removal from wastewater: A review. Crit Rev Environ Sci Technol. 2017;47(19):1836-1876.
13. Aoulad El Hadj Ali Y, Ahrouch M, Ait Lahcen A, Abdellaoui Y, Stitou M. Recent Advances and Prospects of Biochar-based Adsorbents for Malachite Green Removal: A Comprehensive Review. Chemistry Africa. 2022;6(2):579-608.
14. Zhang M, Cheng H, Wang C, Zhou Y. Kaolinite nanotube-stearic acid composite as a form-stable phase change material for thermal energy storage. Applied Clay Science. 2021;201:105930.
15. Chen X, Tremblay AY, Fauteux-Lefebvre C. Controlled kaolinite delamination in urea and surfactant solutions using high-power ultrasonication: impact on platelet morphologies. Applied Clay Science. 2022;228:106640.
16. Vaculíková L, Valovičová V, Plevová E, Napruszewska BD, Duraczyńska D, Karcz R, et al. Synthesis, characterization and catalytic activity of cryptomelane/montmorillonite composites. Applied Clay Science. 2021;202:105977.
17. Samaddar P, Kumar S, Kim K-H. Polymer Hydrogels and Their Applications Toward Sorptive Removal of Potential Aqueous Pollutants. Polymer Reviews. 2019;59(3):418-464.
18. Yang J, Chen Y, Zhao L, Zhang J, Luo H. Constructions and Properties of Physically Cross-Linked Hydrogels Based on Natural Polymers. Polymer Reviews. 2022;63(3):574-612.
19. Hoque M, Alam M, Wang S, Zaman JU, Rahman MS, Johir MAH, et al. Interaction chemistry of functional groups for natural biopolymer-based hydrogel design. Materials Science and Engineering: R: Reports. 2023;156:100758.
20. Azmana M, Mahmood S, Hilles AR, Rahman A, Arifin MAB, Ahmed S. A review on chitosan and chitosan-based bionanocomposites: Promising material for combatting global issues and its applications. Int J Biol Macromol. 2021;185:832-848.
21. Ahmad M, Zhang B, Manzoor K, Ahmad S, Ikram S. Chitin and chitosan-based bionanocomposites. Bionanocomposites: Elsevier; 2020. p. 145-156.
22. Sirajudheen P, Poovathumkuzhi NC, Vigneshwaran S, Chelaveettil BM, Meenakshi S. Applications of chitin and chitosan based biomaterials for the adsorptive removal of textile dyes from water — A comprehensive review. Carbohydr Polym. 2021;273:118604.
23. Laddha H, Jadhav NB, Agarwal M, Gupta R. Enumeration of research journey of MOF@hydrogel composite beads as potential adsorbents for adsorptive elimination of toxic contaminants. Journal of Environmental Chemical Engineering. 2023;11(5):110642.
24. Zhao X, Li P, Zhu J, Xia Y, Ma J, Pu X, et al. Polygonatum polysaccharide modified montmorillonite/chitosan/glycerophosphate composite hydrogel for bone tissue engineering. International Journal of Polymeric Materials and Polymeric Biomaterials. 2021;71(15):1176-1187.
25. Zheng Y, Zhang J, Wang A. Fast removal of ammonium nitrogen from aqueous solution using chitosan-g-poly(acrylic acid)/attapulgite composite. Chem Eng J. 2009;155(1-2):215-222.
26. Mohammadzadeh Pakdel P, Peighambardoust SJ. Review on

recent progress in chitosan-based hydrogels for wastewater treatment application. Carbohydr Polym. 2018;201:264-279.
27. Qi X, Wu L, Su T, Zhang J, Dong W. Polysaccharide-based cationic hydrogels for dye adsorption. Colloids Surf B Biointerfaces. 2018;170:364-372.
28. Khatooni H, Peighambardoust SJ, Foroutan R, Mohammadi R, Ramavandi B. Adsorption of methylene blue using sodium carboxymethyl cellulose-g-poly (acrylamide-co-methacrylic acid)/Cloisite 30B nanocomposite hydrogel. Journal of Polymers and the Environment. 2022;31(1):297-311.
29. Aljeboree AM, Mohammed RA, Mahdi MA, Jasim LS, Alkaim AF. Synthesis, Characterization of P(CH/AA-co-AM) and Adsorptive Removal of Pb (II) ions from Aqueous Solution: Thermodynamic Study. Neuroquantology. 2021;19(7):137-143.
30. Duran S, Şolpan D, Güven O. Synthesis and characterization of acrylamide–acrylic acid hydrogels and adsorption of some textile dyes. Nuclear Instruments and Methods in Physics Research Section B: Beam Interactions with Materials and Atoms. 1999;151(1-4):196-199.
31. Yu M, Liu M. Adsorption of Dyes Using Multi-walled Carbon Nanotube Hydrogel. Chem Res Chin Univ. 2019;35(2):311-318.
32. Stanciu MC, Nichifor M. Influence of dextran hydrogel characteristics on adsorption capacity for anionic dyes. Carbohydr Polym. 2018;199:75-83.
33. Mahdi MA, Jawad AAR, Aljeboree AM, Jasim LS, Alkaim AF. Synthesis, Characterization and Adsorption Studies of a Graphene Oxide/Polyacrylic Acid Nanocomposite Hydrogel. Neuroquantology. 2021;19(9):46-54.
34. Zhu H, Chen S, Duan H, He J, Luo Y. Removal of anionic and cationic dyes using porous chitosan/carboxymethyl cellulose-PEG hydrogels: Optimization, adsorption kinetics, isotherm and thermodynamics studies. Int J Biol Macromol. 2023;231:123213.
35. Mate CJ, Mishra S. Synthesis of borax cross-linked Jhingan gum hydrogel for remediation of Remazol Brilliant Blue R (RBBR) dye from water: Adsorption isotherm, kinetic, thermodynamic and biodegradation studies. Int J Biol Macromol. 2020;151:677-690.